Inorganic Chemistry

including bioinorganic chemistry

August 4, 2014
Volume 53, Number 15
pubs.acs.org/IC

Protonation state controls sulfide binding

Inorganic Chemistry

AUGUST 4, 2014
VOLUME 53 ISSUE 15

INOCAJ 53(15) 7799–8190 (2014)
ISSN 0020-1669
Registered in the U.S. Patent and Trademark Office

ON THE COVER: The protonation state of hydrogen sulfide influences its reactivity with zinc and cobalt phthalocyanines, allowing for chemically reversible sulfide binding. Artwork by Shanna Zentner. See M. D. Hartle, S. K. Sommer, S. R. Dietrich, and M. D. Pluth, p 7800.

Editorial

Communications

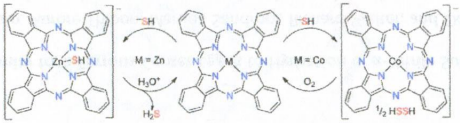

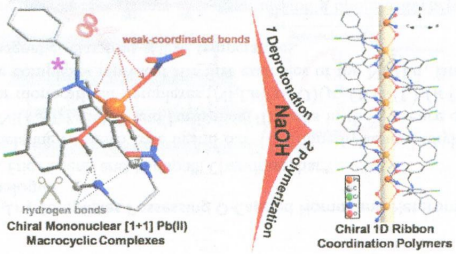

7806 S dx.doi.org/10.1021/ic5012583

Interactions between Anticancer *trans*-Platinum Compounds and Proteins: Crystal Structures and ESI-MS Spectra of Two Protein Adducts of *trans*-(Dimethylamino)(methylamino)dichloridoplatinum(II)

Luigi Messori,* Tiziano Marzo, Elena Michelucci, Irene Russo Krauss, Carmen Navarro-Ranninger, Adoracion G. Quiroga, and Antonello Merlino*

The reactivity of [t-$PtCl_2$(dma)(ma)] with hen egg white lysozyme and bovine pancreatic ribonuclease was investigated by X-ray crystallography and electrospray ionization mass spectrometry. In the resulting adducts, the Pt^{II} center selectively coordinates to histidine or aspartic acid residues, retaining the alkylamino ligands.

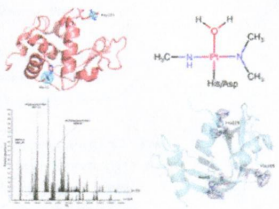

7809 S dx.doi.org/10.1021/ic501310d

Optical Nonlinearity in Cu_2CdSnS_4 and α/β-Cu_2ZnSiS_4: Diamond-like Semiconductors with High Laser-Damage Thresholds

Kimberly A. Rosmus, Jacilynn A. Brant, Stephen D. Wisneski, Daniel J. Clark, Yong Soo Kim, Joon I. Jang, Carl D. Brunetta, Jian-Han Zhang, Matthew N. Srnec, and Jennifer A. Aitken*

Changing Sn^{4+} to Si^{4+} in the I_2–II–IV–VI_4 formula has significant effects on the characteristics critical for nonlinear optical applications. The air-stable, noncentrosymmetric, diamond-like Cu_2CdSnS_4 and α/β-Cu_2ZnSiS_4 exhibit significant second- and third-order nonlinearity. These materials are practical for applications because of their elevated thermal stabilities, wide optical transparency windows, broad regions of phase matchability for second harmonic generation, and high laser-damage thresholds (LDTs). The LDT of the wide-gap α/β-Cu_2ZnSiS_4 surpasses that of commercially available materials.

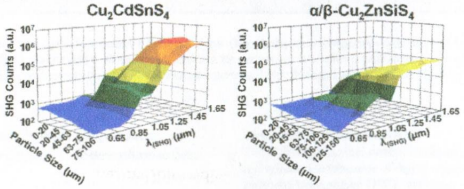

7812 S dx.doi.org/10.1021/ic501509x

Construction and Application of a Rh–Pt DNA Metalloinsertor Conjugate

Alyson G. Weidmann and Jacqueline K. Barton*

We report the synthesis and characterization of a bifunctional DNA metalloinsertor conjugate ("RhPt"). The bimetallic complex contains a rhodium mismatch recognition component tethered to a platinum anticancer agent and exhibits dual binding to DNA involving both metalloinsertion at a base pair mismatch and covalent cross-linking of platinum. In mismatch repair-deficient cells, RhPt exhibits enhanced cellular uptake and cytotoxicity over traditional platinum therapeutics.

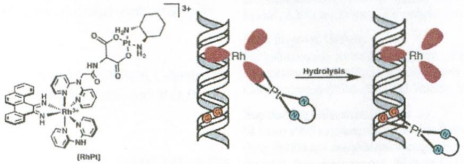

Articles

7837 dx.doi.org/10.1021/ic500135m

Labile or Stable: Can Homoleptic and Heteroleptic PyrPHOS–Copper Complexes Be Processed from Solution?

Daniel Volz, Manuela Wallesch, Stephan L. Grage, Jörg Göttlicher, Ralph Steininger, David Batchelor, Tonya Vitova, Anne S. Ulrich, Clemens Heske, Lothar Weinhardt,* Thomas Baumann,* and Stefan Bräse*

The emission color of Cu(I) complexes is often not the same when comparing bulk samples with thin films, e.g., for organic light-emitting diodes. We investigated if the reason for this is a result of destruction or rather structural distortion for three exemplary complexes with (diphenylphosphino)pyridine derivatives (PyrPHOS)-type ligands.

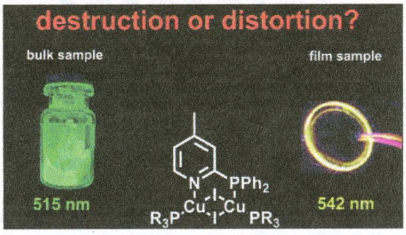

7848 dx.doi.org/10.1021/ic500138w

Influence of a Bridging Group and the Substitution Effect of Bis(1,2,4-triazine) N-Donor Extractants on Their Interactions with a Np^{V} Cation

Xia Yang, Yanni Liang, Songdong Ding, Shoujian Li, Zhifang Chai, and Dongqi Wang*

The equilibrium structures, reaction modes, and bonding characteristics of neptunyl complexes formed with the tridentate bis(triazinyl)pyridines and tetradentate bis(triazinyl)bipyridines and bis(triazinyl)-1,10-phenanthrolines were investigated. It has been shown that neptunyl prefers to complex with tetradentate ligands. Especially, the contribution of an orthophenanthroline bridging group is relatively more pronounced compared to its pyridine counterpart. Density functional theory calculations show that the ligand-exchange reaction assisted by nitrate ions, $[NpO_2(H_2O)_n]^+ + L + NO_3^- \rightarrow NpO_2L(NO_3) + nH_2O$, is the most probable at the interface between water and the organic phase, and the quantum theory of atoms-in-molecules and charge decomposition analysis reveal the main reason responsible for stabilization of the tetradentate ligand complexes.

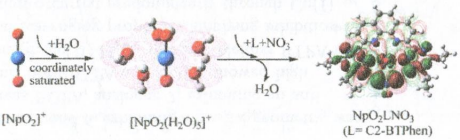

7861 dx.doi.org/10.1021/ic500327s

Technetium and Rhenium Pentacarbonyl Complexes with C_2 and C_{11} ω-Isocyanocarboxylic Acid Esters

Alexander E. Miroslavov,* Yuriy S. Polotskii, Vladislav V. Gurzhiy, Alexander Yu. Ivanov, Alexander A. Lumpov, Margarita Yu. Tyupina, Georgy V. Sidorenko, Peter M. Tolstoy, Daniil A. Maltsev, and Dmitry N. Suglobov

Rhenium(I) and technetium(I) pentacarbonyl complexes with C_2 and C_{11} ω-isocyanocarboxylic acid esters were prepared, fully characterized, and studied to develop a procedure for radiolabeling fatty acids with ^{99m}Tc and $^{188,186}Re$. Rhenium complexes are stable with respect to thermal decarbonylation in ethylene glycol, whereas the technetium complexes undergo slow decarbonylation. On the contrary, in aqueous solutions in the presence of histidine, $[Re(CO)_5(CN(CH_2)COOEt)]ClO_4$ significantly decomposes, whereas its Tc analogue is much more stable.

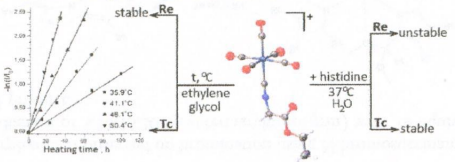

7870 dx.doi.org/10.1021/ic500420u

A Single-Chain Magnet Based on $\{Co^{II}_4\}$ Complexes and Azido/Picolinate Ligands

Jiang Liu, Mei Qu, Mathieu Rouzières, Xian-Ming Zhang,* and Rodolphe Clérac*

A new homonuclear single-chain magnet self-assembles as a one-dimensional coordination network of defective dicubane $\{Co^{II}_4\}$ complexes linked by single Co^{II} ions with the assistance of azido and picolinate ligands. Dominating intrachain ferromagnetic interactions, intrinsic Ising-like Co^{II} anisotropy, and negligible interchain magnetic interactions lead to a thermally activated relaxation time of the magnetization below 8 K.

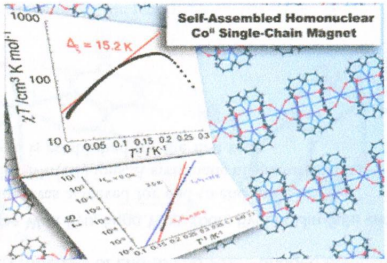

7876 dx.doi.org/10.1021/ic500460n

Selective Synthesis and Redox Sequence of a Heterobimetallic Nickel/Copper Complex of the Noninnocent Siamese-Twin Porphyrin

Lina K. Blusch, Oliver Mitevski, Vlad Martin-Diaconescu, Kevin Pröpper, Serena DeBeer, Sebastian Dechert, and Franc Meyer*

Selective monometalation of the symmetric Siamese-twin porphyrin gave a nickel(II) complex with a vacant dibasic $\{N_4\}$ site. This could be cleanly converted to the homobimetallic dinickel(II) and to the heterobimetallic copper(II)/nickel(II) complexes. Oxidation of the bimetallic systems are largely ligand-based; in the heterobimetallic case, the first oxidation takes place within its Cu-subunit, and the second oxidation then occurs in its Ni-subunit. Redox isomerism upon addition of pyridine, giving nickel(III) species, is reminiscent of known nickel–porphyrin chemistry.

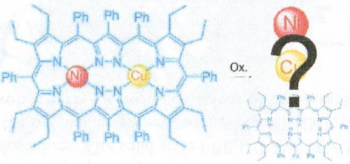

7886 dx.doi.org/10.1021/ic500323r

Thermal- and Light-Induced Spin-Crossover Bistability in a Disrupted Hofmann-Type 3D Framework

Natasha F. Sciortino, Suzanne M. Neville, Jean-François Létard, Boujemaa Moubaraki, Keith S. Murray, and Cameron J. Kepert*

Incorporation of a bent pillar ligand has led to the formation of a novel disrupted Hofmann-type pillared-layer material in which half of the iron(II) centers are spin-crossover-active while the other half are inactive and participate in solvent binding. The material is unusual among systems of this general class in displaying a photomagnetic response.

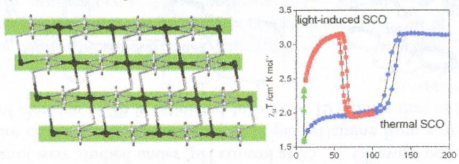

7894 S dx.doi.org/10.1021/ic500468r

Pitfalls in Bromination Reactions of Zinc Porphyrins: Two-Sided Ring Opening of the Porphyrin Macrocycle

Goutam Nandi,* Hatem M. Titi, and Israel Goldberg*

The unusual reactivity of zinc porphyrins is observed on bromination using *N*-bromosuccinamide (NBS) in methanol at reflux. Reaction of [Zn^{II}(por)] (por = dianion of 5,10,15,20-*meso*-tetraarylporphyrin) with 16 equiv of NBS lead to the unexpected two-sided open-ring brominated product.

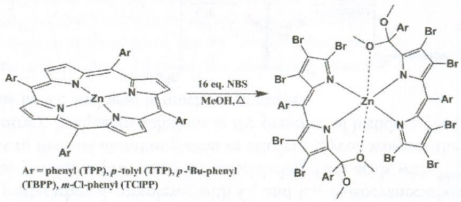

7901 S dx.doi.org/10.1021/ic500465z

Novel Cu(I)-Selective Chelators Based on a Bis(phosphorothioyl)amide Scaffold

Aviran Amir, Alon Ezra, Linda J. W. Shimon, and Bilha Fischer*

In Cu(I)-H_2O_2 system, BTPA, compound **6**, exhibiting a gauche geometry, was a most potent antioxidant, whereas BOPA, analogue **7**, exhibiting an anti geometry, was a poor antioxidant. Both BTPA and BOPA showed high selectivity to Cu(I) vs Fe(II) ion (in Fe(II)-H_2O_2 system). Neither BTPA nor BOPA derivatives showed radical scavenging properties, implying inhibition of the Cu(I)-induced Fenton reaction occurred predominantly through Cu(I) chelation. BTPA analogues are therefore suggested as highly Cu(I) selective lipophilic chelators.

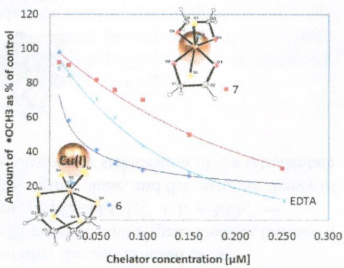

7909 S dx.doi.org/10.1021/ic500599d

Synthesis and Characterization of Two Quaternary Uranium Tellurides, $RbTiU_3Te_9$ and $CsTiU_3Te_9$

Matthew D. Ward, Adel Mesbah, Minseong Lee, Christos D. Malliakas, Eun Sang Choi, and James A. Ibers*

The new solid-state compounds $RbTiU_3Te_9$ and $CsTiU_3Te_9$ have been synthesized and characterized structurally by single-crystal X-ray diffraction methods. The properties of $CsTiU_3Te_9$ have been probed. It is a semiconducting compound of U^{4+}. It shows antiferromagnetic coupling between magnetic U atoms. The very low value of its effective magnetic moment is believed to arise from a coexistence of magnetic and nonmagnetic U atoms.

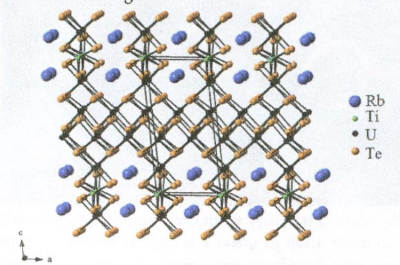

7916 dx.doi.org/10.1021/ic500620k

Cu(II)-Ion-Catalyzed Solvolysis of *N,N*-Bis(2-picolyl)ureas in Alcohol Solvents: Evidence for Cleavage Involving Nucleophilic Addition and Strong Assistance of Bis(2-picolyl)amine Leaving Group Departure

Mei-Ni Belzile, Alexei. A. Neverov, and R. Stan Brown*

The kinetics and products for solvolysis of *N*-*p*-nitrophenyl-*N*′,*N*′-bis(pyridin-2-ylmethyl) urea (**7a**), *N*-methyl-*N*-*p*-nitrophenyl-*N*′,*N*′-bis(pyridin-2-yl methyl) urea (**7b**), and *N*-phenyl-*N*′,*N*′- bis(pyridin-2-yl-methyl) urea (**7c**) promoted by Cu(II) ion in methanol and ethanol were studied under ^{s}pH control at 25 °C. Cleavage occurs to give the *O*-alkyl carbamates of the parent aniline by departure of the Cu(II)-coordinated bis(2-picolyl)amine from a presumed short-lived tetrahedral intermediate. The acceleration of cleavage of **7b** is estimated to be 2×10^{16} times that of the alkoxide-promoted reactions.

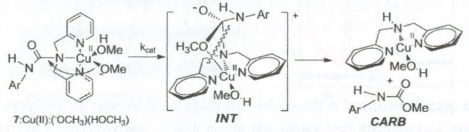

7926 dx.doi.org/10.1021/ic5006743

Unraveling the Polymorphism of [(*p*-cymene)Ru(*κ*N-INA)Cl$_2$] through Dispersion-Corrected DFT and NMR GIPAW Calculations

Davide Presti, Alfonso Pedone,* and Maria Cristina Menziani*

The **1*α***, **1·H$_2$O**, **1*β***, and **1*γ*** crystal forms of [(*p*-cymene)Ru(*κ*N-INA)Cl$_2$] have been structurally investigated by means of periodic dispersion-corrected B3LYP calculations. The solid-state PBE-GIPAW ^{13}C/^{1}H NMR δ_{iso} parameters and ^{13}C spectra are well reproduced. Some revisions to the original assignment of the ^{13}C/^{1}H NMR δ_{iso} parameters of **1·H$_2$O**, **1*β***, and **1*γ*** are proposed, as well as the presence of two COOH···Cl hydrogen bonds of comparable strength in the **1*γ*** polymorph.

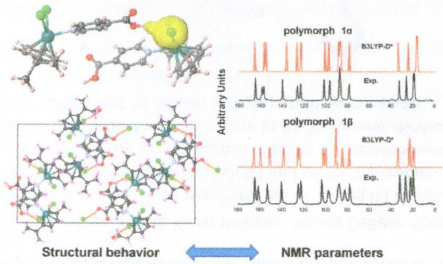

7936 dx.doi.org/10.1021/ic500676k

Synthesis, Structures, and Magnetic Properties of End-to-End Azide-Bridged Manganese(III) Chains: Elucidation of Direct Magnetostructural Correlation

Jeong Hwa Song, Kwang Soo Lim, Dae Won Ryu, Sung Won Yoon, Byoung Jin Suh, and Chang Seop Hong*

Record-high antiferromagnetic coupling was achieved for end-to-end azide-bridged magnetic chains containing Jahn–Teller Mn(III) ions. A systematic magnetostructural relationship based on the torsion angle is established for the first time.

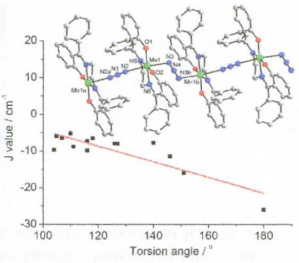

7941 Ⓢ dx.doi.org/10.1021/ic500714h

Corroles That "Click": Modular Synthesis of Azido- and Propargyl-Functionalized Metallocorrole Complexes and Convergent Synthesis of a Bis-corrole Scaffold

Heather L. Buckley, Leah K. Rubin, Mikołaj Chromiński, Brendon J. McNicholas, Katherine H. Y. Tsen, Daniel T. Gryko, and John Arnold*

Bis-corroles have been prepared through a convergent synthesis using a copper-catalyzed azide–alkyne cycloaddition. Synthesis of the final bimetallic complexes has been achieved in three or four steps from commercially available materials in good overall yield. *Meso*-substituted corroles functionalized with a single azido or propargyl group were metalated with copper or iron and attached by Huisgen azide–alkyne cycloaddition ("click" reaction) first to small substrates and then to each other, demonstrating a convergent synthesis of bimetallic bis-corrole molecules.

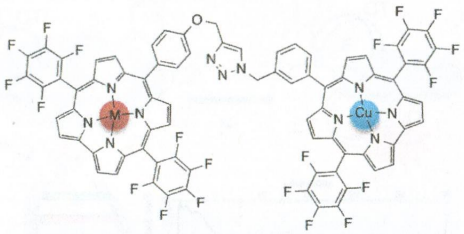

7951 Ⓢ dx.doi.org/10.1021/ic5007428

The Cu^{2+} Binding Properties of Branched Peptides Based on L-2,3-Diaminopropionic Acid

Łukasz Szyrwiel,* Łukasz Szczukowski, József S. Pap, Bartosz Setner, Zbigniew Szewczuk, and Wiesław Malinka

Three *de novo* tetrapeptides built on an L-2,3-diaminopropionic acid branching unit form different copper(II) complexes depending on the ratio of the attached glycine/histidine residues (3/0, 2/1, or 1/2). Comparison of the dominant complex species to those formed with linear peptide fragments as a function of pH reveals that the presence of branching leads to excess stabilization. These results provide a platform for systematic bioinspired activity studies.

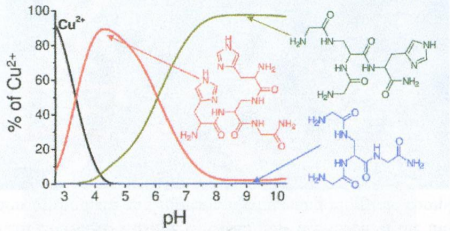

7960 dx.doi.org/10.1021/ic500766t

Synthesis and Characterization of $V^{IV}O$ Complexes of Picolinate and Pyrazine Derivatives. Behavior in the Solid State and Aqueous Solution and Biotransformation in the Presence of Blood Plasma Proteins

Tanja Koleša-Dobravc, Elzbieta Lodyga-Chruscinska, Marzena Symonowicz, Daniele Sanna, Anton Meden, Franc Perdih,* and Eugenio Garribba*

Four picolinate or pyrazine derivatives form with the $V^{IV}O^{2+}$ ion *OC*-6–23 and *OC*-6–24 isomers in the solid state and *OC*-6–23, *OC*-6–24, and *OC*-6–42 in aqueous solution. The interaction with blood proteins results in the formation of $(VO)_2$(apo-hTf) with apo-hTf and $(VO)_x$HSA, VOL_2(HSA), and VOL(HSA)(H_2O) with HSA. The hydrolysis degree at physiological pH affects the biotransformation in the blood.

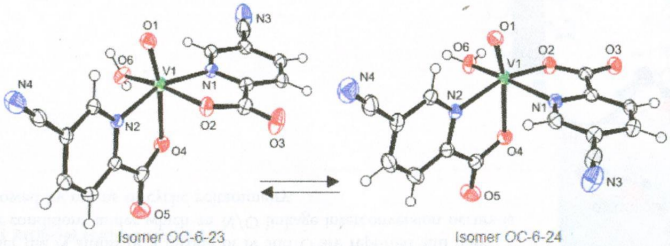

7977 dx.doi.org/10.1021/ic500767f

High-Pressure Polymorph of Phosphorus Nitride Imide HP_4N_7 Representing a New Framework Topology

Dominik Baumann and Wolfgang Schnick*

Reaction of P_3N_5 with NH_4Cl under high-pressure/high-temperature conditions leads to the formation of the new polymorph β-HP_4N_7. Its structure was elucidated using single-crystal diffraction. The compound exhibits an entirely new tetrahedra network structure, which is related to that of recently discovered β-HPN_2.

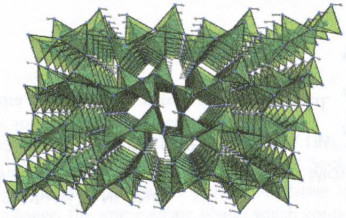

7983 dx.doi.org/10.1021/ic5006715

Probing the Links between Structure and Magnetism in $Sr_{2-x}Ca_xFeOsO_6$ Double Perovskites

Ryan Morrow, John W. Freeland, and Patrick M. Woodward*

The magnetic ground state of A_2FeOsO_6 (A = Sr, Ca) double perovskite compounds can be controlled through application of chemical pressure. Sr_2FeOsO_6 is an antiferromagnetic insulator (T_N = 140, 65 K), but when the larger Sr^{2+} ions are replaced with smaller Ca^{2+} ions to form Ca_2FeOsO_6, a ferrimagnetic (T_C = 350 K) ground state emerges, and the conductivity increases by 4 orders of magnitude. This behavior is explained in terms of competing superexchange interactions.

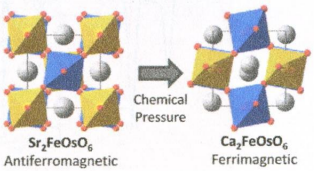

7993 S

dx.doi.org/10.1021/ic5007814

Copper(I) and Copper(II) Uranyl Heterometallic Hybrid Materials

Zhehui Weng, Zhi-hui Zhang, Travis Olds, Marcin Sterniczuk, and Peter C. Burns*

Hydrothermal methods provide both Cu(II) and Cu(I) uranyl organic frameworks with isonicotinic acid ligands. Frameworks are facilitated by ligand saturation of the isonicotinic acid in the Cu(I) compound, and in the Cu(II) compound by incorporation of a uranyl ion oxygen into the Cu(II) coordination octahedron.

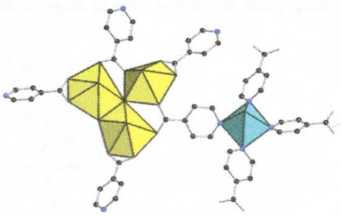

7999 S

dx.doi.org/10.1021/ic5008523

$Ru[(bpy)_2(dppz)]^{2+}$ and $Rh[(bpy)_2(chrysi)]^{3+}$ Targeting Double Strand DNA: The Shape of the Intercalating Ligand Tunes the Free Energy Landscape of Deintercalation

Duvan Franco, Attilio V. Vargiu, and Alessandra Magistrato*

Metadynamics simulations with Path-Collective-Variable elucidate how the shape of the intercalating ligands tunes the free energy landscape for deintercalation of rhodium and ruthenium containing inorganic complexes from double strand DNA.

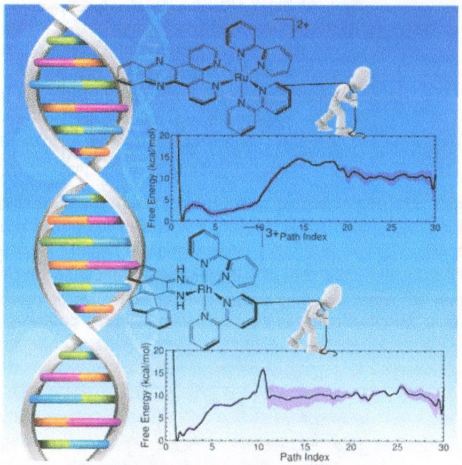

8009 S dx.doi.org/10.1021/ic500880m

Tetra-2,3-pyrazinoporphyrazines with Externally Appended Pyridine Rings. 15. Effects of the Pyridyl Substituents and Fused Exocyclic Rings on the UV–Visible Spectroscopic Properties of Mg(II)–Porphyrazines: A Combined Experimental and DFT/TDDFT Study

Maria Pia Donzello,* Giorgia De Mori, Elisa Viola, Claudio Ercolani, Giampaolo Ricciardi, and Angela Rosa*

The triad of Mg^{II} porphyrazine macrocycles [Py_8PzMg], [$Py_8PyzPzMg$], and [$Py_8QxPzMg$], all sharing as common structural features the presence of externally appended 2-pyridyl rings, was examined by UV–visible measurements. The observed spectral changes along the series were interpreted by DFT/TDDFT calculations.

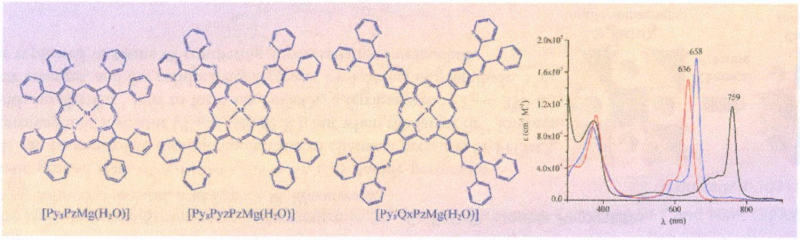

8020 S dx.doi.org/10.1021/ic500881v

Cation Exchange in a 3D Perovskite—Synthesis of $Ni_{0.5}TaO_3$

Midori Amano Patino, Thomas Smith, Weiguo Zhang, P. Shiv Halasyamani, and Michael A. Hayward*

Reaction of $NiCl_2$ with $NaTaO_3$ leads the formation of the perovskite phase $Ni_{0.5}TaO_3$, via a topochemical nickel-for-sodium cation exchange in which the framework of apex-linked TaO_6 octahedra present in the parent phase is retained.

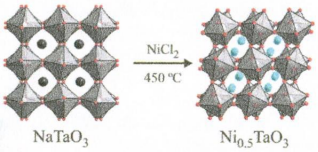

8025 S dx.doi.org/10.1021/ic5009076

Synthesis, Characterization, and Linkage Isomerism in Mononuclear Ruthenium Complexes Containing the New Pyrazolate-Based Ligand Hpbl

Laia Francàs, Rosa M. González-Gil, Albert Poater, Xavier Fontrodona, Jordi García-Antón, Xavier Sala,* Lluís Escriche,* and Antoni Llobet*

New mononuclear Ru complexes containing the Hpbl hemilabile ligand that can coordinate by either the N atoms or a mixing of N and O are reported and fully characterized. The conditions under which an N/O linkage interconversion occurs is described and followed by means of cyclic voltammetry.

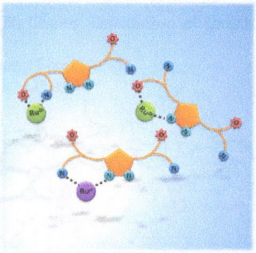

8036 dx.doi.org/10.1021/ic500944t

Sensitizing Tb(III) and Eu(III) Emission with Triarylboron Functionalized 1,3-Diketonato Ligands

Larissa F. Smith, Barry A. Blight, Hee-Jun Park, and Suning Wang*

Triarylboryl functionalized 1,3-diketonato ligands have been found to be effective in sensitizing Ln(III) ion emission. By controlling the location of the boryl unit on the diketonato ligand, selective sensitization of Eu(III) or Tb(III) ion has been achieved. Fluoride ions have been found to act as a switch in these systems, turning on the emission of the Eu(III) ion and turning off the emission of the Tb(III) ion.

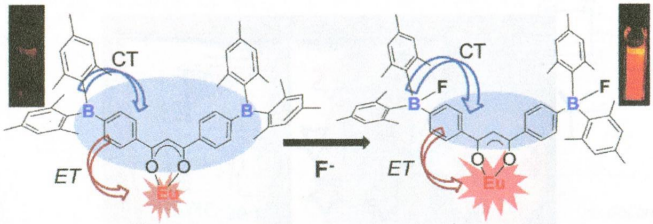

8045 dx.doi.org/10.1021/ic501041h

Enhanced Near-Infrared to Visible Upconversion Nanoparticles of Ho^{3+}-Yb^{3+}-F^- Tri-Doped TiO_2 and Its Application in Dye-Sensitized Solar Cells with 37% Improvement in Power Conversion Efficiency

Jia Yu, Yulin Yang,* Ruiqing Fan,* Danqing Liu, Liguo Wei, Shuo Chen, Liang Li, Bin Yang, and Wenwu Cao*

We have designed and fabricated NIR-to-green upconversion fluorescent nanoparticles of Ho^{3+}-Yb^{3+}-F^- tridoped TiO_2 as an advanced upconversion material for making more efficient DSSCs. An overall conversion efficiency of 10.00% was achieved when this upconversion material was introduced into the bilayer-structured photoanode, which is associated with closer attachment of the *in situ* upconversion process, enhanced light harvesting, and photogenerated electron−hole pair separation as well as elevated Femi level.

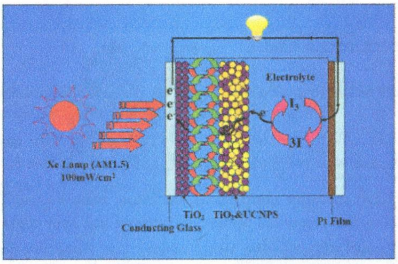

8054 dx.doi.org/10.1021/ic501026k

Solvent-Dependent Switch of Ligand Donor Ability and Catalytic Activity of Ruthenium(II) Complexes Containing Pyridinylidene Amide (PYA) N-Heterocyclic Carbene Hybrid Ligands

Vivienne Leigh, Daniel J. Carleton, Juan Olguin, Helge Mueller-Bunz, L. James Wright,* and Martin Albrecht*

A chelating hybrid ligand containing a pyridinylidene amide (PYA) and a N-heterocyclic carbene donor site adapts its donor ability in response to the solvent medium, comprising either a π-acidic imine neutral resonance form or a strongly σ-donating mesoionic resonance form of the PYA unit. These differences in donor ability have direct implications for redox and catalytic applications.

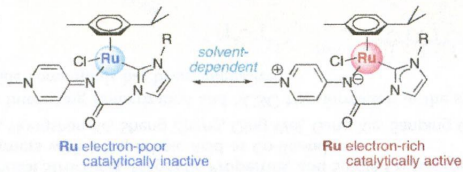

8061 S dx.doi.org/10.1021/ic5010598

Bis-Heteroleptic Ruthenium(II) Complex of a Triazole Ligand as a Selective Probe for Phosphates

Bijit Chowdhury, Snehadrinarayan Khatua, Ranjan Dutta, Sourav Chakraborty, and Pradyut Ghosh*

A weakly luminescent ruthenium complex, $\mathbf{1}(PF_6)_2$, acts as an "OFF-ON" molecular switch toward sensing of $H_2PO_4^-/HP_2O_7^{3-}$, and the first solid-state structural evidence of dihydrogenpyrophosphate recognition via solitary C–H··· anion interactions is demonstrated.

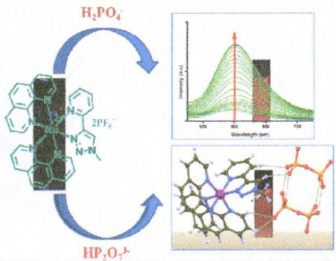

8071 S dx.doi.org/10.1021/ic501014c

Cobaloxime-Based Artificial Hydrogenases

Marine Bacchi, Gustav Berggren, Jens Niklas, Elias Veinberg, Michael W. Mara, Megan L. Shelby, Oleg G. Poluektov, Lin X. Chen, David M. Tiede, Christine Cavazza, Martin J. Field, Marc Fontecave, and Vincent Artero*

Two artificial hydrogenases have been prepared through insertion of the cobaloxime moieties $\{Co(dmgH)_2\}$ and $\{Co(dmgBF_2)_2\}$ ($dmgH_2$ = dimethylglyoxime) in apo *Sperm-whale* myoglobin. Both biohybrids exhibit the catalytic activity for H_2 evolution in near-neutral aqueous conditions.

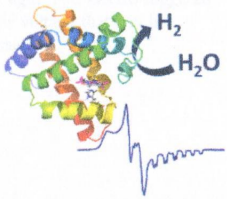

8083 S dx.doi.org/10.1021/ic501069x

Ion-Exchange Mechanism of Layered Transition-Metal Oxides: Case Study of $LiNi_{0.5}Mn_{0.5}O_2$

Hyeokjo Gwon, Sung-Wook Kim, Young-Uk Park, Jihyun Hong, Gerbrand Ceder, Seokwoo Jeon,* and Kisuk Kang*

The ion exchange in $NaNi_{0.5}Mn_{0.5}O_2$ is not a simple two-phase process but rather involves several intermediate complex compounds. In the early stage of ion exchange, the intermediate phase, which contains randomly distributed sodium and lithium ions in the lithium layers, forms almost immediately, with extremely fast exchange kinetics. Successively, a rather slower two-phase conversion occurred, involving a structural shuffling process.

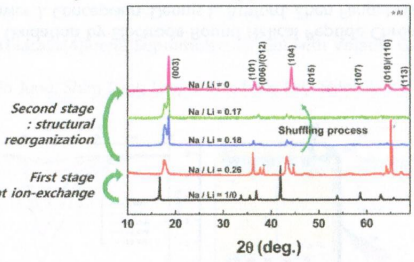

8088 (S) dx.doi.org/10.1021/ic5010769

Solvent-Induced Syntheses, Crystal Structures, Magnetic Properties, and Single-Crystal-to-Single-Crystal Transformation of Azido-Cu(II) Coordination Polymers with 2-Naphthoic Acid as Co-ligand

Xiangyu Liu, Peipei Cen, Hui Li, Hongshan Ke, Sheng Zhang, Qing Wei, Gang Xie, Sanping Chen,* and Shengli Gao

Solvent-induced effect leads to interesting isomerization and SCSC transformation in the system of copper-azido-naphthoic acid. Magnetism for the Cu-azide compounds has been emphasized.

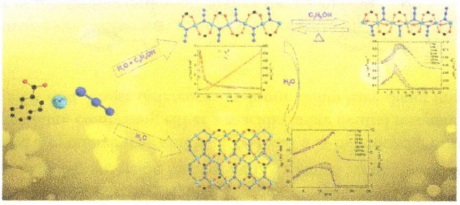

8098 (S) dx.doi.org/10.1021/ic501089f

$Na_4La_2(CO_3)_5$ and $CsNa_5Ca_5(CO_3)_8$: Two New Carbonates as UV Nonlinear Optical Materials

Min Luo, GenXiang Wang, Chensheng Lin, Ning Ye,* Yuqiao Zhou, and Wendan Cheng

Introducing rare earth and alkaline earth into the alkaline carbonate generates two novel UV nonlinear optical materials $Na_4La_2(CO_3)_5$ and $CsNa_5Ca_5(CO_3)_8$ with similar structures that exhibit different SHG effects.

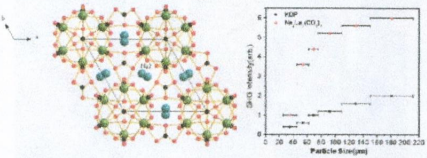

8105 (S) dx.doi.org/10.1021/ic5011083

2D Cd(II)–Lanthanide(III) Heterometallic–Organic Frameworks Based on Metalloligands for Tunable Luminescence and Highly Selective, Sensitive, and Recyclable Detection of Nitrobenzene

Shu-Ran Zhang, Dong-Ying Du, Jun-Sheng Qin, Shun-Li Li, Wen-Wen He, Ya-Qian Lan,* and Zhong-Min Su*

A family of novel 2D isostructural Cd(II)–lanthanide(III) heterometallic–organic frameworks **IFMC-36-Eu$_x$Tb$_y$** based on metalloligands was constructed by introducing the desired Eu(III) and Tb(III) contents. **IFMC-36-Eu$_x$Tb$_y$** exhibits multicolor emissions ranging from red to green. Particularly, **IFMC-36-Eu** displays highly selective, sensitive, and recyclable properties in sensing nitrobenzene. It is the first time that a d–f heterometallic–organic framework can be utilized as fluorescent sensor to detect nitrobenzene in the systems with complicated components.

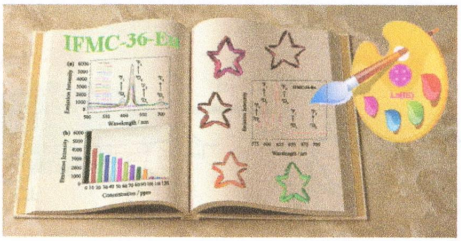

8114 S dx.doi.org/10.1021/ic501127d

$Y(IO_3)_3$ as a Novel Photocatalyst: Synthesis, Characterization, and Highly Efficient Photocatalytic Activity

Hongwei Huang,* Ying He, Ran He, Zheshuai Lin, Yihe Zhang,* and Shichao Wang

The novel $Y(IO_3)_3$ photocatalyst exhibits a photocatalytic activity much higher than that of commercial TiO_2 (P25) for photodegradation of rhodamine B. The excellent photocatalytic performance of $Y(IO_3)_3$ should be ascribed to the its very positive valence band position, which endows it with a very strong photooxidation ability to produce abundant •OH radicals as active species.

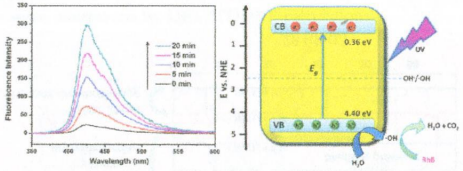

8120 S dx.doi.org/10.1021/ic5011488

Synthesis and Electrocatalytic Water Oxidation by Electrode-Bound Helical Peptide Chromophore–Catalyst Assemblies

Derek M. Ryan, Michael K. Coggins, Javier J. Concepcion, Dennis L. Ashford, Zhen Fang, Leila Alibabaei, Da Ma, Thomas J. Meyer,* and Marcey L. Waters*

Herein, we describe a general modular synthetic strategy for making chromophore–water-oxidation catalyst assemblies using late-stage assembly of the catalyst, and we evaluate their electrocatalytic water oxidation when surface-bound to FTO. We find that the assemblies exhibit greater than 10-fold rate enhancements compared to the homogeneous catalyst alone. This synthetic strategy allows for systematic optimization of the chromophore, catalyst, and scaffold, addressing a significant challenge in the field.

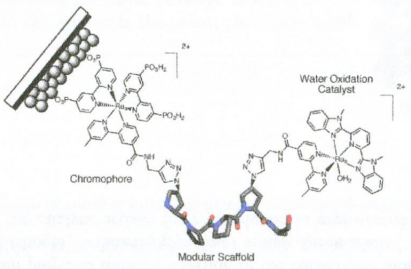

8129 S dx.doi.org/10.1021/ic5011902

Enhanced Spin-Crossover Behavior Mediated by Supramolecular Cooperative Interactions

Zheng Yan, Jin-Yan Li, Tao Liu, Zhao-Ping Ni,* Yan-Cong Chen, Fu-Sheng Guo, and Ming-Liang Tong*

The magnetic behaviors of three one-dimensional coordination polymers $[Fe^{II}(L)_2(AgCN)_2]$ were modulated from paramagnetic to abrupt and hysteretic SCO near room temperature through adjustment of the electronic substituent effect and intermolecular interactions.

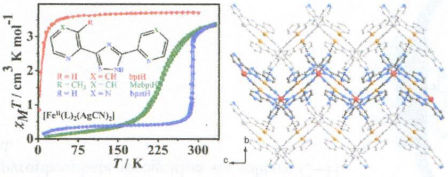

8136 dx.doi.org/10.1021/ic501211f

Structures, Vibrational Frequencies, and Stabilities of Halogen Cluster Anions and Cations, $X_n^{+/-}$, n = 3, 4, and 5

K. Sahan Thanthiriwatte, Jason M. Spruell, David A. Dixon,* Karl O. Christe, and H. Donald B. Jenkins

The energetics of the homonuclear polyhalogen ions, X_3^+, X_3^-, X_4^+, X_4^-, X_5^+, and X_5^- (X = Cl, Br, I), have been calculated using the Feller–Peterson–Dixon approach for the prediction of reliable enthalpies of formation. The stabilities of the ions with respect to loss of X_2 for n = 3 and 5 show that X_3^+ are stable and that X_3^-, X_5^+, and X_5^- are marginally stable even at low temperatures.

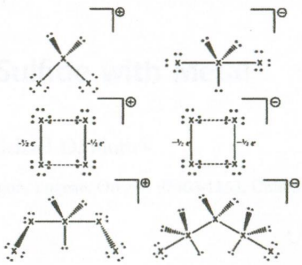

8147 dx.doi.org/10.1021/ic5012154

Molecular Iron(III) Phosphonates: Synthesis, Structure, Magnetism, and Mössbauer Studies

Joydeb Goura, Prasenjit Bag, Valeriu Mereacre,* Annie K. Powell, and Vadapalli Chandrasekhar*

Tetra- and pentanuclear iron(III) phosphonate cages $[Fe_4(t\text{-}BuPO_3)_4(HphpzH)_4]\cdot 5CH_3CN\cdot 5CH_2Cl_2$ and $[HNEt_3]_2[Fe_5(\mu_3\text{-}O)(\mu\text{-}OH)_2(Cl_3CPO_3)_3(HphpzH)_5(\mu\text{-}phpzH)]\cdot 3CH_3CN\cdot 2H_2O$ have been synthesized and characterized.

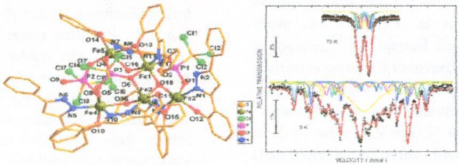

8155 dx.doi.org/10.1021/ic501219q

Synthesis of a "Super Bulky" Guanidinate Possessing an Expandable Coordination Pocket

Arnab K. Maity, Skye Fortier,* Leonel Griego, and Alejandro J. Metta-Magaña

The synthesis and full characterization of the "super bulky" guanidinate $[(Ar^*N)_2C(R)]^-$ [$[^{Ar*}$**ketguan**$]^-$; Ar* = 2,6-bis(diphenylmethyl)-4-*tert*-butylphenyl and R = $NC(^tBu)_2$] are presented. Examination of its coordination profile with group 1 cations reveals a highly encumbering yet very flexible ligand scaffold.

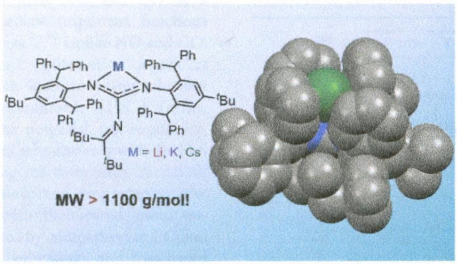

8165 Ⓢ dx.doi.org/10.1021/ic501226v

Molecular Magnetic Investigation of a Family of Octanuclear $[Cu_6Ln_2]$ Nanoclusters

Shufang Xue, Yun-Nan Guo, Lang Zhao, Haixia Zhang, and Jinkui Tang*

A remarkable new family of octanuclear Cu−Ln molecular nanomagnets represents an efficient model to probe magnetic exchange interactions, relaxation dynamics, and magnetic caloric effects.

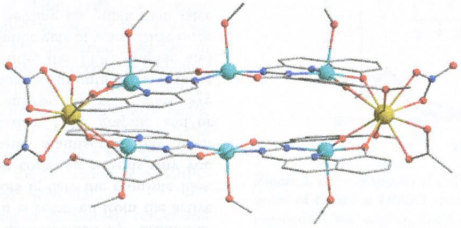

8172 Ⓢ dx.doi.org/10.1021/ic5013044

Diarylethene-Containing Carbon-Rich Ruthenium Organometallics: Tuning of Electrochromism

Yifei Liu, Cheikh Mbacké Ndiaye, Corinne Lagrost,* Karine Costuas,* Sylvie Choua, Philippe Turek, Lucie Norel, and Stéphane Rigaut*

The association of a DTE photochromic unit with ruthenium acetylides provides sophisticated light- and electro-triggered switches featuring multicolor electrochromism and electrochemical cyclization at remarkably low voltage that can be manipulated owing to the noninnocent behavior of the carbon-rich ligands in the redox processes.

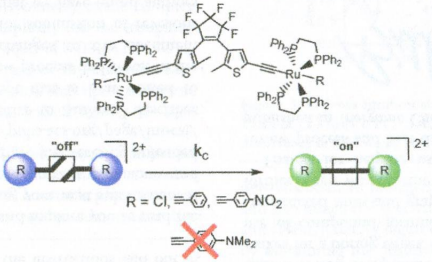

Additions and Corrections

8189 dx.doi.org/10.1021/ic501602e

Correction to Geometric Change of Thiacalix[4]arene Supramolecular Gel with Volatile Gases and Its Chromogenic Detection for Rapid Analysis

Ka Young Kim, Sunhong Park, Sung Ho Jung, Shim Sung Lee, Ki-Min Park, Seiji Shinkai, and Jong Hwa Jung*

Ⓢ Supporting Information available via online article